IEEE Access
Multidisciplinary | Rapid Review | Open Access Journal

Received 4 September 2022, accepted 29 October 2022, date of publication 3 November 2022, date of current version 9 November 2022.

Digital Object Identifier 10.1109/ACCESS.2022.3219211

RESEARCH ARTICLE

Research on Dynamic Control Method of Loom Spindle Braking System Based on Fuzzy Neural Network

YANJUN XIAO[1,2,3], XIAOLIANG WANG[3], YUE ZHAO[3], AND WEILING LIU[3]

[1]School of Mechanical Engineering, Tianjin Key Laboratory of Power Transmission and Safety Technology for New Energy Vehicles, Hebei University of Technology, Tianjin 300401, China
[2]Career Leader Intelligent Control Automation Company, Suqian, Jiangsu 223800, China
[3]School of Mechanical Engineering, Hebei University of Technology, Tianjin 300401, China

Corresponding authors: Yanjun Xiao (xyj_hebut@163.com) and Weiling Liu (weiling20220000@163.com)

This work was supported in part by the Jiangsu Province Training Fund under Grant BRA2020244.

ABSTRACT Aiming at the problems of slow response speed of loom electromagnetic braking system and low accuracy of parking angle after braking, resulting in driving marks and thin and dense roads of fabrics, a braking control system based on fuzzy theory and back propagation (BP) neural network is proposed to improve the response speed and control accuracy of the braking system. Firstly, the transmission torque in the braking process of the loom is dynamically analyzed by establishing the mathematical model of electromagnetic braking and the Ansoft electromagnetic finite element model. The causes of braking angle slip are explored, and the driving mechanism of the electromagnetic clutch control circuit based on PWM pulse is analyzed. Based on the control strategy of excitation current, by introducing the fuzzy theory and BP neural network, a fuzzy electromagnetic braking control system based on a neural network is proposed to improve the adaptive ability of the system. At the same time, the improved bat algorithm (IBA-BP) algorithm is used to train the neural network to avoid the generation of local optimization and improve the control accuracy of the system. The simulation and experimental results show that compared with PID control and fuzzy PID control, the neural network method based on fuzzy theory has a smaller braking slip angle, and the accuracy of parking angle after braking action is less than 10 °, which improves the control accuracy of loom electromagnetic braking system and weaving quality.

INDEX TERMS Fuzzy theory, neural network, bat algorithm, electromagnetic braking, loom.

I. INTRODUCTION

With the continuous development of the textile industry, the loom, as the most important piece of equipment in the textile industry, the automation process and intelligence of its control system have become the key factors affecting fabric quality. With the application of electronic and computer technology in the loom's working module, the loom's production efficiency and stability are significantly improved [1], [2]. The continuous weaving process of the loom results from the cooperation of multiple process nodes, especially the effective cooperation between the braking process and weaving sequence, and the control accuracy of braking will directly affect the quality of fabric and weaving efficiency. With the wide application of electromagnetic technology in industrial automation, the structure of the loom braking system has also changed, from the early full mechanical braking mode to the electromagnetic braking mode combining automation and mechanization of electronic technology. The emergence of the electromagnetic clutch is of great significance to the brake control of the loom. It has a compact structure and easy to realize automatic control, which has significantly improved the brake response of the loom. At the same time, it is possible to accurately and effectively control the braking process through modern control technology.

In the weaving process of the loom, when the loom stops due to artificial braking or failure, how to ensure the accuracy of the loom stop has an important impact on the quality of

The associate editor coordinating the review of this manuscript and approving it for publication was Hongwei Du.

fabric. The braking process of the loom refers to that the electromagnetic clutch realizes the clutch and braking of the loom by absorbing and separating the friction plate through electromagnetic attraction under the control of current [3]. Therefore, the braking angle can be effectively controlled directly by adjusting the working state of the electromagnetic clutch. However, in the weaving process, affected by the loom process sequence, the moment of inertia of the loom spindle changes regularly with the rotation angle of the spindle. Therefore, the load on the loom spindle changes dynamically, which leads to the fluctuation of braking slip angle under different braking angles, resulting in problems such as start-up marks and uneven weft density, which will directly affect the fabric quality and make the next loom start-up complex. Secondly, the electromagnetic clutch depends on the on-off of the coil to control the engagement and separation of the clutch, which makes the response time lag of the electromagnetic clutch when braking. The response time of the master-slave rotor of the electromagnetic clutch and the spindle inertia and load force during the sliding friction of the friction plate result in the different slip amount of the braking angle at different spindle speeds. Therefore, its control system has the characteristics of multivariable and time lag. Due to the change of force when the spindle runs to different angles and the complexity of the braking process of the electromagnetic clutch, the traditional feedback algorithm is difficult to control the braking slip angle accurately. At the same time, due to the nonlinearity of the electromagnetic clutch driving circuit and the strong interference of the loom running in a complex environment, it is difficult to meet the requirements of system nonlinearity and variable parameters by using conventional control methods [4].

Both classical and modern control theories are based on the accurate modeling of the target, such as classical PID control, modern adaptive control, and other methods, which can achieve the expected control effect [5], [6]. Conventional PID control is widely used in industrial control because of its simple structure, high reliability, and easy engineering implementation. However, it is difficult to establish an accurate model due to the complexity and uncertainty of the electromagnetic clutch control process. The limitations of the traditional control theory which relies too much on the accurate mathematical model are gradually reflected. Therefore, when the system is highly nonlinear and uncertain, it is often difficult to achieve a good control effect only by adjusting a single PID parameter [7]. Zhao et al. [8] applied the fuzzy PID control strategy to the automobile electromagnetic braking system. By considering the nonlinearity and time variation of the braking system, the current in the electromagnetic braking coil is controlled to realize the accurate adjustment of the braking force. Compared with fuzzy control and PID control, the fuzzy PID strategy can effectively reduce the braking time and shorten the braking distance. Wang et al. [9] proposed a fuzzy control strategy of electromagnetic clutch based on particle swarm optimization (PSO) optimization. The optimized quantization factor tracks the parameter change of the fuzzy controller in real-time with the change of environment and load to improve the robustness and control accuracy of the controller. The simulation and experimental results show that the fuzzy control algorithm based on PSO can effectively reduce the slip and the impact degree compared with the traditional fuzzy control algorithm. Wu et al. [10] designed a magnetic particle clutch current controller to solve the nonlinear problem of the magnetic particle clutch driving circuit and used a genetic algorithm to adjust PID control parameters. The simulation results show that the driving control dynamics of tuning PID based on a genetic algorithm is better than that of traditional PID control, and the system adaptability is better. Claudia-Adina et al. [11] proposed a fuzzy modeling method of a nonlinear servo system represented by an electromagnetic clutch system. The T-S fuzzy model based on the modal equivalence principle is used to realize the linearization process of the nonlinear model. The simulation results verify the effectiveness of the fuzzy model of the electromagnetic clutch system. Chen et al. [12] proposed an electric vehicle electromagnetic braking controller based on fuzzy reasoning to improve the performance of the ABS braking system and keep the braking slip ratio in the best range. Experiments verify the rationality of this method. Li et al. [13] because of the nonlinearity of the electromagnetic clutch drive circuit and the difficulty of PID control in realizing dynamic control parameter setting, an intelligent control method of fuzzy PID control is proposed and simulated in a Matlab environment. The simulation results show that compared with the traditional PID control, the electromagnetic clutch driven by this method has a fast current dynamic response, small overshoot and high steady-state accuracy. In addition, adaptive control, synovial control and other control methods have also been applied in electromagnetic clutch [14], [15]. Compared with the PID control strategy, fuzzy control has strong robustness and can meet the control requirements of complex processes such as nonlinearity and parameter uncertainty. However, it should be pointed out that using the fuzzy rule table to fuzzy infer the input variables to obtain the control parameters and realize online self-tuning can improve the accuracy of the controller to a certain extent and have better flexibility. However, its membership function and fuzzy control rules depend on expert experience and have great subjectivity and uncertainty. Wu et al. [16] to solve the problem that it is difficult to achieve optimal control when using traditional PID control for the electromagnetic clutch in a complex environment, an online tuning of PID control parameters based on radial basis function neural network is proposed. Through the improvement, the anti-interference ability of the electromagnetic clutch is improved and has better adaptability. Yazdanpanah et al. [17] proposed a robust speed and slip control scheme for a hybrid electromagnetic brake (HEB) system based on a neural network for uncertain system parameters and unknown external disturbance conditions. The controller does not need accurate information about braking, and the control algorithm can effectively track the performance and ensure the stability

of the closed-loop system. Pramudijanto et al. [18] used a fuzzy neural network in the anti-lock electromagnetic braking system to control the wheel slip value. Neural networks are based on fuzzy mechanisms, that is, through the process of fuzzification, reasoning and defuzzification, the fuzzy neural network controller can reduce the overshoot response by 43.2%. Quan et al. [19] established the controller of the electromagnetic braking system of agricultural motor vehicles based on a fuzzy neural network, and used genetic algorithm to optimize the fuzzy rules, increase the braking torque, and control the slip rate in a small range. The above research shows that compared with fuzzy control or PID control, neural network algorithms further improve the control accuracy of the electromagnetic clutch braking system. Although the neural network has strong self-learning and adaptive ability, it can only describe the complex functional relationship between many data and can not use system information and expert knowledge. Therefore, combining fuzzy control theory and neural networks may be a more effective solution [20]. With the proposal of fuzzy neural network (FNN) theory, it has been widely used in complex control engineering [21], [22], [23], [24]. Although fuzzy neural networks have been widespread, their application and research in loom braking systems are still rare. A fuzzy neural network combines the learning mechanism of a neural network and the language reasoning ability of the fuzzy system, but like other neural networks, the acquisition of its model depends on the training of the learning algorithm. However, the traditional BP algorithm has some defects, such as slow convergence speed and easily falling into local optimization, making it difficult to meet the accuracy requirements of complex control systems. Therefore, the research and improvement of the neural network learning algorithm is also a problem to be explored in this paper. The main innovations of this paper are as follows:

1. The dynamic analysis of the braking process of the electromagnetic clutch is carried out, and the influence of the response hysteresis and the driving circuit on the braking performance of the loom is clarified through the electromagnetic simulation analysis.
2. According to the time-varying and nonlinear characteristics of loom braking, a dynamic control system based on fuzzy neural network is established by using the fusion method of fuzzy theory and neural network.
3. By introducing IBA algorithm, the training parameters of neural network are optimized, the defect of easily falling into local optimization caused by a single BP algorithm is improved, and the performance of neural network model is improved.

The rest of this paper is organized as follows: the second section analyzes the braking principle of the loom. In the third section, the mathematical modeling and simulation of the electromagnetic braking process are carried out, and the factors affecting braking accuracy are studied. The fourth section describes the control strategy. The fifth section verifies the control strategy through simulation and experiment and analyzes the experimental results. The sixth section summarizes the work done.

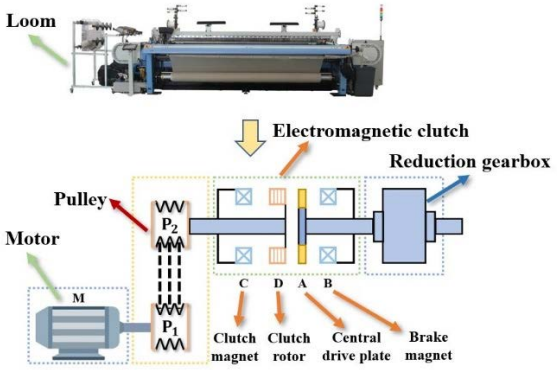

FIGURE 1. Structure diagram of loom electromagnetic clutch.

II. ELECTROMAGNETIC BRAKING PRINCIPLE OF LOOM

The electromagnetic clutch used in the loom is a friction plate clutch. When the electromagnetic clutch is energized, the armature generates suction and the spring releases pressure. Or spring pressurization and electromagnetic pressure relief can transfer torque between friction plates to produce a braking effect [25], [26]. The electromagnetic clutch system in the loom is mainly composed of four basic components: central drive plate A, brake magnet B, clutch magnet C and clutch rotor D. C and A are engaged to form an electromagnetic clutch, and B and A are engaged to form an electromagnetic brake. P1 and m are connected by a shaft, the movement between P1 and P2 is connected by a triangular belt, D and P2 are connected by a hard shaft. P1, P2 and D rotate together driven by the motor, as shown in Fig. 1.

When the electromagnetic clutch is energized, the motor M, pulley P1, pulley P2 and clutch rotor D operate. When the start key is pressed, the coil of clutch magnet C is energized to generate electromagnetic suction. The drive plate A is drawn to clutch rotor D. A and D absorb the friction torque and accelerate together until the speed is the same, D drives the crankshaft and reduction wheelset to run together through A. at this time, the loom is in operation. When the loom needs to stop for some reason during normal operation, the clutch magnet coil C loses power and the brake magnet coil B is powered on and engaged. At this time, the electromagnetic force generated by the coil current of B draws A to the end face of B while B is fastened on the base by the iron core. Through the friction resistance moment, the rotating shaft of the loom stops quickly. At this time, the whole machine stops.

III. DYNAMIC ANALYSIS OF ELECTROMAGNETIC BRAKING

A. DYNAMIC MODEL OF ELECTROMAGNETIC BRAKING

The transmission torque M of the electromagnetic clutch is determined by the friction force between the driving and driven plates. In addition to the friction area and friction

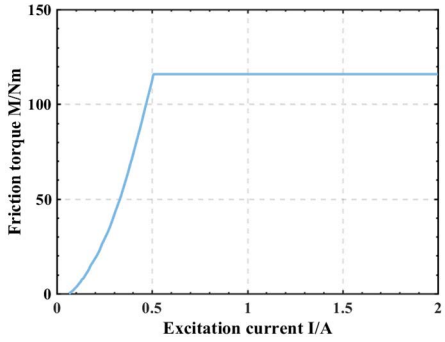

FIGURE 2. Simulation model and characteristic curve of the relationship between M and I.

coefficient, the friction force mainly depends on the pressing force F between the driving and driven plates. The expression of transmission torque of electromagnetic clutch is:

$$M = \mu R_m F\,(m-1) \tag{1}$$

where μ is the friction coefficient, F is the electromagnetic suction of the clutch, m is the number of friction plates, R_m is the effective radius of the friction surface. According to formula (1), the transmission torque M of the clutch is related to the friction coefficient, friction area and the pressing force of the clutch. When the clutch structure is certain, μ, R_m, m is the determined value, and the vertical pressure on the yoke is the vertical attraction on the armature. Therefore, the characteristic of electromagnetic suction F is the characteristic of clutch transmission torque M. The electromagnetic suction F of the armature can be obtained by the following formula:

$$F = 10\left(\frac{B}{5000}\right)^2 S \tag{2}$$

$$B = \frac{0.4\pi IW}{(1+\sigma)(n-1)\delta} \tag{3}$$

where B is the effective magnetic induction intensity, I is the excitation current, and W is the number of coil turns, σ is the magnetic flux leakage coefficient, δ is the clearance between friction plates, and n is the number of friction plates. According to formulas (2) and (3), it can be seen that for the selected electromagnetic clutch, its parameters W, σ, δ, n are determined. Therefore, the magnitude of the electromagnetic attraction force F is only related to the excitation current I. To obtain the relationship between the transmission torque M and the excitation current I of the electromagnetic clutch, the corresponding relationship curve is obtained through MATLAB simulation, as shown in Fig. 2. The friction coefficient of the electromagnetic clutch is $\mu = 0.5$, the excitation coil $W = 1300$, and the effective radius of the friction surface $R_m = 0.048m$, the magnetic leakage coefficient $\sigma = 1.2$, and the gap between the friction plates $\delta = 0.04cm$.

From the characteristic curve of the relationship between the friction torque M and the excitation current I shown in Fig. 2, it can be found that when the current is small, the armature of the electromagnetic clutch cannot attract, so no torque is generated. When the excitation current increases to a certain value, the friction torque M of the clutch is in a positive proportional linear relationship with the excitation current I. When the excitation current increases to a certain value, the friction torque M of the clutch remains constant. For the electromagnetic clutch, the greater the excitation current I, by the greater the pull-in force F, the faster the pull-in speed of the clutch armature, and the greater the output torque, thereby improving the speed of starting and stopping of the loom and the stopping accuracy. Therefore, to improve the loom braking speed and make the clutch output torque adjustable, it can be realized by changing the excitation current of the clutch coil.

Ansoft finite element simulation model is established to calculate and simulate the engagement process of an electromagnetic brake. The engagement process of the electromagnetic clutch is mainly divided into two stages. In the first stage, the current of the electromagnetic clutch coil increases to a stable state, and the suction in this process is insufficient to make the armature move. In the second stage, when the suction generated by the coil current is large enough, the armature moves in the gap due to the suction and finally accelerates with the friction plate. When the coil is energized, the change rate of inductance L with time is 0. The current increases exponentially, and the corresponding formula is:

$$i = \frac{U}{R}\left(1 - e^{-\frac{t}{T}}\right) \tag{4}$$

where U is the electromagnetic clutch coil voltage, R is the coil resistance, t is the power on time, and T is the time constant. The movement of the friction disc in the electromagnetic clutch will change the length of the gap, resulting in a change in the magnetic conductivity of the gap. The change of inductance and electromagnetic force in the dynamic process can be expressed as:

$$L(x) = W^2 \frac{\gamma S}{x} \tag{5}$$

$$F = \frac{(Wi)^2 \gamma S}{2x^2} \tag{6}$$

where γ is the permeability, s is the cross-sectional area of the magnetic circuit, I is the coil current, W is the number of coil turns, and x is the dynamic gap length. During the braking process of the electromagnetic clutch, the change rate of the flux linkage is:

$$\frac{d\Psi}{dt} = L(x)\frac{di}{dt} + \frac{dL}{dx}\frac{dx}{dt}i \tag{7}$$

When the armature moves due to suction, the friction disc is quickly compressed with the brake disc to produce friction torque, resulting in a braking effect. If the air and friction resistance is ignored, the mechanical motion equation can be obtained:

$$F = m\frac{dv(x)}{dt} \tag{8}$$

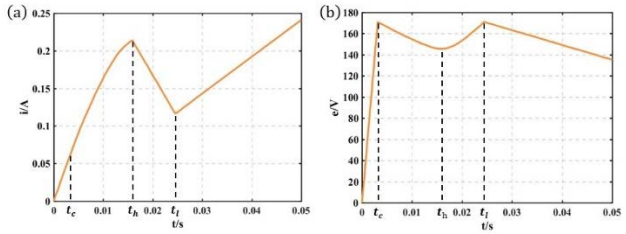

FIGURE 3. The relationship between the variation curve of current and back EMF in the coil and time.

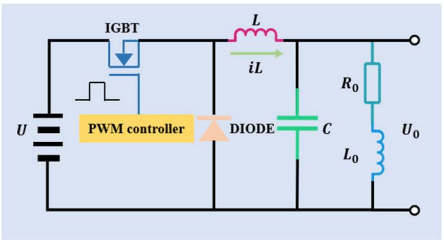

FIGURE 4. Electromagnetic clutch drive circuit.

where F is the electromagnetic suction, m is the mass of the brake disc, and $v\,(x)$ is the moving speed of the brake disc in the vertical direction.

Due to the small excitation current in the early stage, the clutch is at a time t_c start braking, the friction disc moves, and the current continue to increase. During this period, the reverse electromotive force in the coil increases, $i\frac{dL}{dx}\frac{dx}{dt}$ increases, and the self-induced electromotive force $L\frac{di}{dt}$ decreases. At this time, the movement speed is low, the back electromotive force is small, and the current growth decreases. With the increase of back EMF and motion speed, the current decreases after point t_h. From the highest point t_h to point t_l the absolute value of the motion back EMF increases, but the direction changes, causing the current to decrease. The friction disc is fully combined with the brake disc at the point t_h, and the friction speed is zero. Since the motion back EMF is zero, the current begins to increase according to a new law until it is stable. The simulation results of the variation curves of current and back EMF in the coil are shown in Fig. 3.

Through the analysis of the above simulation results, it can be seen that the electromagnetic brake has a time lag in response. The time used in $0 \sim t_h$ a period is the pull-in lag time of the electromagnetic clutch, which is an important factor causing brake angle slip. According to the experimental results in Fig. 3, the pull-in lag time of the electromagnetic clutch is about $17ms$, the loom spindle speed of this control system is $500rad/min$, and the angle that the main shaft rotates during the pull-in delay time of the electromagnetic clutch is 51°. However, due to spindle load fluctuation and other factors, the actual lag angle usually deviates from the ideal value. Many parking experiments on site show that the rotation angle of the spindle from the beginning of parking to the completion of parking is 65°. Therefore, it is necessary to start the electromagnetic clutch 65° in advance to achieve accurate braking control.

B. ELECTROMAGNETIC BRAKE DRIVE CIRCUIT

The loom brake control system needs to have a fast response capability. For the electromagnetic clutch, the greater the excitation current, the greater the transmission torque, and the faster the pull in response. This characteristic has been proved in the simulation results in Fig 2. The electromagnetic brake control system designed in this paper is divided into two parts: rectification and voltage regulation. The main function of the rectifier part is to convert the AC input of the power grid into DC output, and the main function of the voltage regulating part is to convert the DC output of the rectifier part into the required voltage and load it to both ends of the electromagnetic coil. In this paper, the step-down circuit based on IGBT is used as the power driving circuit of the loom electromagnetic clutch, and its principle structure diagram is shown in Fig. 4. The excitation coil of the electromagnetic clutch is equivalent to R_0L_0 series. The circuit is mainly composed of power switching device IGBT, energy storage inductance L, filter capacitor C, freewheeling diode and equivalent parts of excitation coil.

When the PWM signal is at a high level, the switch IGBT is turned on, the diode is turned off, and the power supply U at the input end transmits the power to the load and increases the inductive current. The period of the PWM signal is T, and the duration of high and low levels in a cycle are t_{on} and t_{off}. During the conduction time, the inductance current increment is:

$$\Delta L_+ = \int_0^{t_{on}} \frac{U - U_0}{L} dt \tag{9}$$

When the PWM signal is at low level, the switch IGBT is turned off, the diode is turned on, and the inductance current drops. The reduction amount is:

$$\Delta L_- = \int_{t_{on}}^{T} \frac{U_0}{L} dt \tag{10}$$

When the circuit is in steady state, the inductive current i_L must be repeated periodically. The increase of inductance current during IGBT on is equal to the decrease of inductance current during IGBT off, that is, $\Delta L_+ = \Delta L_-$. The relationship between output voltage and input voltage can be obtained as follows:

$$U_0 = \frac{t_{on}}{t_{on} + t_{off}} U = \frac{t_{on}}{T} U = dU \tag{11}$$

The average value of the current passing through the solenoid coil in a switching cycle is I_d. The equivalent resistance of the solenoid coil is R_0, then from formula (11):

$$I_d = \frac{U_0}{R_0} U = \frac{dU}{R_0} \tag{12}$$

The circuit structure changes with the switch on and off, and the circuit equation also changes with the switch on and

off, so the ideal switch model is time-varying. Thus, the state equation of the circuit shown in Figure 4 can be written as:

$$\begin{cases} \dfrac{di_L(t)}{dt} = \dfrac{1}{L}\left[u(t) - u_0(t)\right], & t \in [0, dT] \\ \dfrac{du_0(t)}{dt} = \dfrac{1}{C}\left[i_L(t) - \dfrac{u_0(t)}{R_0}\right], & t \in [0, dT] \end{cases} \tag{13}$$

$$\begin{cases} \dfrac{di_L(t)}{dt} = \dfrac{1}{L}\left[-u_0(t)\right], & t \in [dT, T] \\ \dfrac{du_0(t)}{dt} = \dfrac{1}{C}\left[i_L(t) - \dfrac{u_0(t)}{R_0}\right], & t \in [dT, T] \end{cases} \tag{14}$$

According to the respective state equations and the proportion of time when the switch is in the on state and off state, the approximate average state equation of the system in a switching cycle can be obtained as follows:

$$\frac{d}{dt}\begin{bmatrix} \langle i_L(t)\rangle \\ \langle u_0(t)\rangle \end{bmatrix} = \begin{bmatrix} 0 & -\frac{1}{L} \\ \frac{1}{c} & -\frac{1}{RC} \end{bmatrix}\begin{bmatrix} \langle i_L(t)\rangle \\ \langle u_0(t)\rangle \end{bmatrix} + dt\begin{bmatrix} \frac{1}{L} \\ 0 \end{bmatrix}\langle u(t)\rangle \tag{15}$$

When the converter operates at a certain static operating point, the DC components corresponding to the state variable and the input variable are $\langle i_L(t)\rangle = I_L$, $\langle u_0(t)\rangle = U_0$ and $\langle u(t)\rangle = U$ respectively, and the steady-state duty cycle $d(t) = D$. The static operating point is obtained by taking into formula (15):

$$\frac{U_0}{U} = D, I_L = \frac{DU}{R} \tag{16}$$

The small signal state equation can be obtained by combining the state equation and static operating point with the introduction of disturbance method as follows:

$$\frac{d}{dt}\begin{bmatrix} \hat{i}_L(t) \\ \hat{u}_C(t) \end{bmatrix} = \begin{bmatrix} 0 & -\frac{1}{L} \\ \frac{1}{C} & -\frac{1}{RC} \end{bmatrix}\begin{bmatrix} \hat{i}_L(t) \\ \hat{u}_C(t) \end{bmatrix} + \begin{bmatrix} \frac{D}{L} \\ 0 \end{bmatrix}\hat{u}(t) + \begin{bmatrix} \frac{U}{L} \\ 0 \end{bmatrix}\hat{d}(t) \tag{17}$$

Through Laplace transform, the transfer function between the control of the converter and the output voltage can be calculated as:

$$G(s) = \frac{\hat{u}_0(s)}{\hat{d}(s)} = \frac{U_0}{d}\frac{1}{1 + s\frac{L}{R} + s^2LC} = \frac{48}{1 + 5.69 \times 10^{-3}s + 44.4 \times 10^{-6}s^2} \tag{18}$$

As a PWM controller, STM32F103 single-chip microcomputer calculates the duty cycle that should be output to the backward channel circuit according to the internal program, and the output PWM pulse controls the on and off of the IGBT by driving the isolation circuit. By adjusting the duty ratio d, the average voltage U_0 across the load is changed, so as to realize the control of the coil current of the electromagnetic clutch, and then adjust the transmission torque during the braking process of the electromagnetic brake.

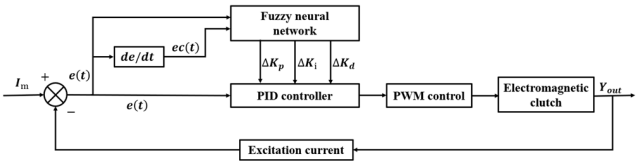

FIGURE 5. Fuzzy neural network PID controller structure.

IV. CONTROLLER DESIGN

A. FUZZY NEURAL NETWORK CONTROLLER

The neural network has strong self-learning and adaptive ability and can approach all complex nonlinear systems. Fuzzy control can easily obtain the expert knowledge expressed by language. The combination of the two fuzzy neural networks can endow the neural network with the ability of reasoning and induction, make the nodes and parameters of the neural network have clear physical significance, and make the fuzzy control have the ability of self-learning. Fuzzy theory is used to enhance the data processing ability of the neural network to focus on fuzzy information. The neural network is used to improve the fuzzy rules in the fuzzy control system, and the membership function is optimized accordingly. Therefore, combining fuzzy theory and neural network is applied to the parameter tuning of the PID controller in this paper. The fuzzy neural network PID controller structure is shown in Fig. 5.

In order to ensure the accuracy of the braking angle of the loom, real-time control of the current passing through the electromagnetic clutch coil is required. Input I_m is the current information of the given electromagnetic clutch coil. The deviation e between the excitation current of the electromagnetic clutch and I_m collected by the current sensor and the change rate ec of the excitation current deviation are used as the input of the fuzzy neural network. Take ΔK_p, ΔK_i, ΔK_d as the output and transmit it to the PID controller, and the PID controller outputs the error signal. Through real-time comparison with the sawtooth wave signal of the PWM controller, the duty ratio d of the output signal is dynamically adjusted to ensure that the electromagnetic brake works under the predetermined conditions. The transfer function of PID controller is shown in formula (19), and the system can reach a better control state by adjusting three parameters K_p, K_i and K_d.

$$G_c(s) = K_p + \frac{K_i}{s} + K_d s \tag{19}$$

The expression of the online control law is:

$$\begin{cases} K_p(k) = K_p(k-1) + \Delta K_p \\ K_i(k) = K_i(k-1) + \Delta K_i \\ K_d(k) = K_d(k-1) + \Delta K_d \end{cases} \tag{20}$$

where, ΔK_p, ΔK_i, and ΔK_d are the initial values of proportional, integral and differential, respectively, which can be obtained by engineering setting method, $K_p = 80$, $K_i = 20$, $K_d = 0.0002$. Set the basic universe of input and output

TABLE 1. Domain corresponding table of input and output parameters.

Input and output parameters	Fuzzy domain	Quantification factor	Basic domain
e	[-0.3,-0.2,-0.1,0,0.1,0.2,0.3]	1	[-0.3, 0.3]
e_c	[-0.3,-0.2,-0.1,0,0.1,0.2,0.3]	10	[-0.03, 0.03]
$\triangle K_p$	[-3, -2, -1,0,1,2,3]	0.1	[-30, 30]
$\triangle K_i$	[-3, -2, -1,0,1,2,3]	0.2	[-15, 15]
$\triangle K_d$	[-0.03,-0.02,-0.01,0,0.01,0.02,0.03]	200	[-0.00015, 0.00015]

parameters of the fuzzy neural network, and select certain quantitative factors. The fuzzy universe corresponding to each parameter is shown in Table 1.

The values in the fuzzy universe in Table 1 are transformed into fuzzy subsets $\{NB, NM, NS, ZO, PS, PM, PB\}$. The elements in the subsets correspond to negative large, negative medium, negative small, zero, positive small, positive medium and positive large, respectively. Secondly, the fuzzy subset of each fuzzy variable is defined, that is, the shape of the membership function of the fuzzy subset is determined. The membership function uses the Gaussian function. In the fuzzification process, the exact quantity needs to be transformed into the corresponding fuzzy universe. The quantization factor K_e of system error and the quantization factor K_{ec} of error change rate are respectively determined by the following formula:

$$\begin{cases} E = e \times K_e \\ EC = ec \times K_{ec} \end{cases} \tag{21}$$

In addition, the control quantity obtained by the fuzzy control algorithm must be transformed into the basic domain required by the controlled object to obtain the accurate control quantity.

$$\begin{cases} \Delta K_p = K_p \times G_{K_p} \\ \Delta K_i = K_i \times G_{K_i} \\ \Delta K_d = K_d \times G_{K_d} \end{cases} \tag{22}$$

where, K_p, K_i, K_d is the exact control quantity obtained by the decision of fuzzy set in the fuzzy universe of control quantity, ΔK_p, ΔK_i, ΔK_d is an exact quantity in the basic universe, $G_{K_p}, G_{K_i}, G_{K_d}$ is the scale factor.

The fuzzy neural network based on the Mamdani model is adopted in this paper. The structure of the fuzzy neural network model is shown in Fig. 6. It is a five-layer feedforward neural network with two inputs and three outputs. By taking the excitation current deviation e and deviation change rate ec as the input of the fuzzy neural network, after the fuzzification, fuzzy reasoning and rule normalization of the three hidden layers in the middle, the output layer defuzzizes and calculates the previous layer to obtain the corresponding PID control correction parameter ΔK_p, ΔK_i, ΔK_d. The functions of each layer of the fuzzy neural network and the input-output relationship between each layer are as follows.

The first layer is the input layer. Each node of this layer is directly connected with the input variable, and each node

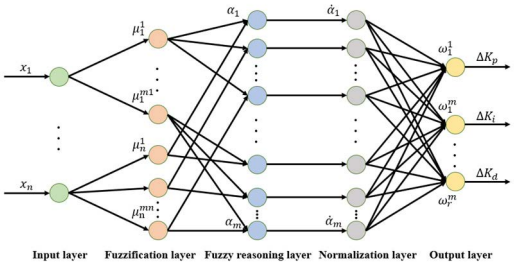

FIGURE 6. Fuzzy neural network structure.

represents an input variable. There are two neuron nodes in the input, which are the deviation $x_1 = e$ and deviation change rate $x_2 = ec$.

$$\begin{cases} I_i^{(1)} = x_i \\ O_{ij}^{(1)} = I_i^{(1)} \end{cases} \tag{23}$$

where, I and O are network layer input and output respectively, $I = 1, 2, j = 1, 2, \ldots, 7$.

The second layer is the fuzzification layer, which is mainly used to calculate the membership value of each input component. Through the input variable x_i fuzzy segmentation, get its corresponding language variable value and divide the input variable into 7 language variables. The membership value $f_{ij}(x_i)$ of x_i variable is calculated by using the membership function. Among, the membership function adopts the Gaussian function. There are 14 nodes in this layer, and each node represents the membership value of a language variable.

$$\begin{cases} I_i^{(2)} = O_{ij}^{(1)} \\ O_{ij}^{(2)} = f_{ij}(x_i) = e^{-\frac{(x_i - c_{ij})^2}{\sigma_{ij}^2}} \end{cases} \tag{24}$$

where, c_{ij} is the center of the membership function, σ_{ij} is the width of the membership function.

The third layer is the fuzzy reasoning layer, which has 49 nodes, each corresponding to a fuzzy rule. In this layer, the fitness $\alpha_l (l = 1, 2, \ldots, 49)$ of each fuzzy rule is obtained after calculating the membership value of each variable to determine the matching status of fuzzy rules.

$$\begin{cases} I_i^{(3)} = O_{ij}^{(2)} \\ O_l^{(3)} = \alpha_l = \prod_{i=1}^{2} \prod_{j=1}^{7} f_{ij}(x_i) \end{cases} \tag{25}$$

The fourth layer is the normalization layer, which normalizes the overall network structure. The nodes are the same as in the previous layer.

$$\begin{cases} I_l^{(4)} = O_l^{(3)} \\ O_l^{(4)} = \bar{\alpha_l} = \dfrac{\alpha_l}{\sum_{l=1}^{49} \alpha_l} \end{cases} \tag{26}$$

The fifth layer is the output layer, which is used to solve the fuzzy quantity obtained by fuzzy reasoning and obtain the final output of the fuzzy neural network. There are three

nodes in this layer, which correspond to three control correction parameters ΔK_p, ΔK_i and ΔK_d of PID controller, respectively.

$$\begin{cases} I_l^{(5)} = O_l^{(4)} \\ O_h^{(5)} = y_h = \sum_{h=1}^{3} \sum_{l=1}^{49} \omega_{hl} \bar{\alpha}_l \end{cases} \tag{27}$$

where y_h is the output of the network, ω_{hl} is the connection weight between the normalization layer and the output layer, $h = 1, 2, 3$.

After the above tuning, the parameter value of PID can be obtained, and the increment of the incremental PID controller can be obtained as:

$$\begin{aligned} \Delta U_k = {} & K_p[e(k) - e(k-1)] + K_i e(k) \\ & + K_d (e(k) - 2e(k-1) + e(k-2)) \end{aligned} \tag{28}$$

Based on the topology of the fuzzy neural network, we can see the learning process of the fuzzy neural network, that is, by constantly adjusting the network parameters to obtain the optimal fuzzy control rules and weight parameters. Among them, the adjustment of fuzzy control rules can be realized by optimizing the central value and width of the membership function. The parameters to be learned by the fuzzy neural network are mainly the central value c_{ij}, width σ_{ij} and connection weight ω_{hl} of membership function. These parameters usually need to be obtained by training the neural network through learning algorithms, and different learning algorithms often have different training effects. Therefore, we need to select the appropriate algorithm to achieve a better control effect.

B. IBA-BP ALGORITHM

As a commonly used learning algorithm of the fuzzy neural network, the BP algorithm has the ability of precise optimization. It makes the output of the network and the expected value as close as possible to achieve the purpose of approximation by constantly modifying the weight value of the network. The objective cost function ε is defined as:

$$\varepsilon = \frac{1}{2} (y_m(n) - y_o(n))^2 \tag{29}$$

where, $y_m(n)$ represents the expected output of the fuzzy neural network, $y_o(n)$ represents the actual output. To minimize the mean square error, it is necessary to continuously adjust the free parameters of the fuzzy neural network and optimize the parameters through the gradient descent method. The parameter learning algorithm is shown below.

$$\begin{cases} c_{ij}(n+1) = c_{ij}(n) - \beta \dfrac{\partial \varepsilon}{\partial c_{ij}} + \alpha[c_{ij}(n) - c_{ij}(n-1)] \\ \sigma_{ij}(n+1) = \sigma_{ij}(n) - \beta \dfrac{\partial \varepsilon}{\partial \sigma_{ij}} + \alpha[\sigma_{ij}(n) - \sigma_{ij}(n-1)] \\ \omega_{hl}(n+1) = \omega_{hl}(n) - \beta \dfrac{\partial \varepsilon}{\partial \omega_{hl}} + \alpha[\omega_{hl}(n) - \omega_{hl}(n-1)] \end{cases} \tag{30}$$

where α is the inertia coefficient, β is the learning rate of c_{ij}, σ_{ij} and ω_{hl}.

The traditional BP algorithm is an optimization method of local search. The weight of its network is gradually adjusted along the direction of local improvement, which will make the algorithm fall into the local extremum, resulting in the failure of network training. Because the essence of the BP algorithm is the gradient descent method, the sawtooth phenomenon is bound to appear in the process of optimizing the objective function, which makes the BP algorithm inefficient and slow convergence speed. Because of the defects of the BP algorithm, the traditional solution is to use the mainstream optimization algorithms, such as genetic algorithm (GA), particle swarm optimization (PSO) algorithm, and simulated annealing algorithm (SA), to optimize its initial value [27], [28], [29]. Although the above optimization algorithm has a certain degree of feasibility, there is room for improvement in optimization ability, convergence, stability, etc. Yang [30] proposed the optimization algorithm of the Bat algorithm (BA) in 2010. Compared with the traditional heuristic algorithm, this algorithm has better global optimization ability. Therefore, in recent years, the Bat algorithm has been used to optimize the neural network model to obtain higher training accuracy [31], [32], [33]. Under ideal conditions, the algorithm successfully hunts food by changing the frequency f, loudness A_i, and pulse firing rate r_i emitted by the bat during foraging to locate the prey or obstacle. Each bat is in position x_i have a random flight speed v_i. At the same time, it has different frequencies, loudness and pulse emissivity. When hunting and discovering prey, bats choose the best solution by changing the frequency, loudness and pulse emissivity until the target stops or the conditions are met.

$$\begin{cases} f_t = f_{min} + (f_{max} - f_{min})\beta \\ v_i^t = v_i^{t-1} + \left(x_i^t - x_*\right) f_i \\ x_i^t = x_i^{t-1} + v_i^t \end{cases} \tag{31}$$

where $\beta \in [-1, 1]$ is a random vector, x_* is the optimal global solution at time t. The algorithm strengthens the search near the optimal global solution, constantly generates new solutions and looks for the optimal solution. The search method is:

$$x_{new} = x_{old} + \mu A^t \tag{32}$$

where $\mu \in [-1, 1]$ is a random number, and A^t is the average loudness of the group at time t. In the expansion stage, to search a wider space and produce high pitch intensity, bats gradually reduce the search space and use stronger frequency and small sound intensity to fine position with the progress of the search and the determination of the approximate orientation of the optimal solution. The frequency and intensity of sound waves emitted by bats are calculated as follows:

$$\begin{cases} r_i^{t+1} = r_i^0[1 - e^{-\gamma t}] \\ A_i^{t+1} = \alpha A_i^t \end{cases} \tag{33}$$

where $\alpha \in (0, 1)$, is the acoustic loudness attenuation coefficient. $\gamma > 0$ is the pulse frequency enhancement coefficient.

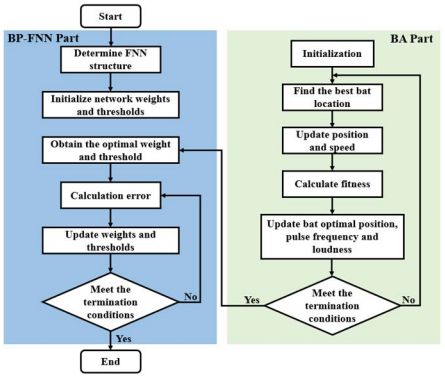

FIGURE 7. IBA-BP algorithm flow chart.

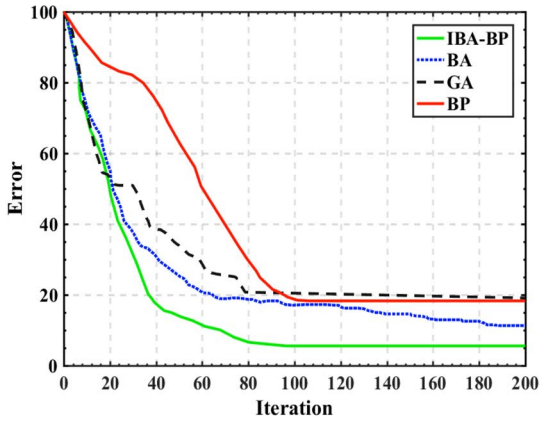

FIGURE 8. Comparison of convergence errors under different algorithms.

r_i^0 is the initial pulse frequency of bat i. When and only when the bat's position is optimized, the loudness and frequency of the pulse will be updated, indicating that the bat is moving towards the best position.

In this paper, the fusion algorithm of the BA algorithm and BP algorithm is used to optimize the parameters of the fuzzy neural network. In the initial stage of fuzzy neural network training, the BA algorithm is used to globally optimize the parameter values, prioritize obtaining the approximate optimal solution of network weight parameters, and then use the BP algorithm for later iteration to obtain more ideal parameter values. However, it should be pointed out that although the bat algorithm has good optimization ability, the search speed coefficient of the basic algorithm is always 1 in the search process, which greatly reduces the population diversity and individual flexibility. It is straightforward to lead to an imbalance between global search and local search. Therefore, by introducing the weight coefficient ω And adjusting factor c to improve the optimization accuracy of the algorithm. The updated bat flight speed formula is:

$$\begin{cases} v_i^{t+1} = \omega v_i^t + \left(x_* - x_i^t\right) f_i + \left(x_{i*} - x_i^t\right) c \\ \omega = \omega_{max} - \left(\omega_{max} - \omega_t\right) \dfrac{N_{max} - N_t}{N_{max}} + \omega_e \end{cases} \tag{34}$$

$$\omega_i^t = \begin{cases} 1.2 \times \omega_i^t, & iff\ \left(x_i^t\right) \le f\left(x_i^{t-1}\right) \\ 0.2 \times \omega_i^t, & else \end{cases} \tag{35}$$

where weight $\omega \in (0, 1)$, ω_t is the initial value of the weight, ω_{max} is the maximum weight, ω_e is the weight change value. The expression of adjustment factor c is:

$$c = c_{min} + \left(c_{max} - c_{min}\right) \frac{\omega - \omega_{max}}{\omega_{max} - \omega_{min}} \tag{36}$$

where the adjustment factor $c \in (1, 2)$. The adjustment factor can reduce the weight of bats faraway from food so that these bats far away from the target will not make the population tend to local optimization. After completing the improvement of the BA algorithm, the IBA-BP algorithm is used to train the fuzzy neural network. The flow of the IBA-BP algorithm is shown in Fig. 7.

V. EXPERIMENT AND SIMULATION

A. ELECTROMAGNETIC BRAKING ALGORITHM TEST

To verify the effectiveness of this algorithm, the FNN model is constructed. By selecting the same parameter setting and initial value, the IBA-BP algorithm, BP algorithm, and GA are used to train FNN. The structure of FNN is set as 2-14-49-49-3, the population size is set as 50, and the maximum number of iterations is 200. f_{min} and f_{max} is 0 and 2, respectively, the maximum pulse intensity A_0 is 1, and the adjustment parameters of loudness and pulse $\alpha = \gamma = 0.8$, $\omega_t = 1$, $\omega_e = 1$, $\omega_{max} = 1$, learning factor $c_{min} = 1.2$. The error convergence comparison of the experimental results is shown in Fig. 8.

It can be seen from Fig. 8 that under the condition of 200 iterations, the convergence speed of the BP algorithm in the early stage of training is slow, and it converges when iterating 100 times. GA algorithm has a fast convergence speed in the early stage, but with iteration's progress, it falls into local optimization and is difficult to converge to high accuracy. BA algorithm maintains almost the same convergence speed as GA and IBA in the early stage. However, there is still the problem of the local or global optimal solution in the late iteration stage, resulting in the difficult balance of searchability, poor stability and slow convergence speed. IBA-BP algorithm has the fastest convergence speed in the early stage. IBA algorithm is used in the early stage of iteration. After about 40 iterations, the error has decreased significantly, and the parameter range of the neural network has been basically determined. At this time, the BP algorithm is used to complete the subsequent training, and finally, the training error tends to be stable in about 80 iterations. Compared with BP, GA, and BA, the IBA-BP algorithm can achieve higher convergence accuracy at the end of the iteration. The fuzzy inference rules trained by the IBA-BP algorithm are shown in Fig. 9.

The simulation experiment is carried out on the trained FNN model, and the simulation results of IBA-FNN PID are compared with Fuzzy PID and PID control algorithms. In the simulation, the PID parameter is $K_p = 80$, $K_i = 20$, $K_d = 0.0002$. The input signal is a stepping signal with an

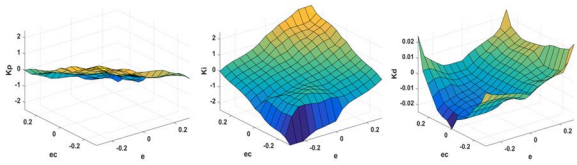

FIGURE 9. Fuzzy inference rules.

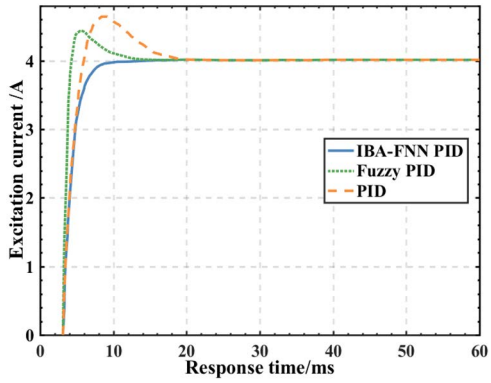

FIGURE 10. Step response curve.

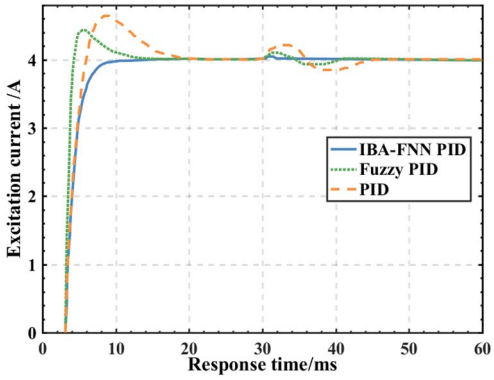

FIGURE 11. Step response curve under disturbance.

amplitude of 4, and the output is the value calculated by PID, Fuzzy PID and IBA-BP- FNN PID.

It can be seen from Fig. 10 that under the traditional PID control, the system rises slowly, the adjustment time is long, and the overshoot reaches 16%, while excessive overshoot is likely to cause fabric quality problems in the braking control. When Fuzzy PID control is adopted, the control effect is improved and the rise time is greatly reduced, but the overshoot is still 11%. In contrast, when IBA-FNN PID is used for control, the overshoot of the system is almost zero. Although the rise time is increased compared with Fuzzy PID due to the increase in algorithm complexity, it is still much better than traditional PID control. The adjustment time is greatly reduced and the control performance is greatly improved.

Further, to verify the anti-interference ability of the algorithm, a disturbance signal with an amplitude of 0.5 is applied

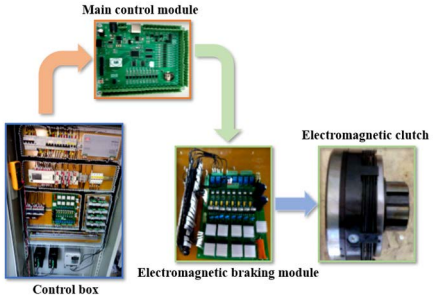

FIGURE 12. Loom electromagnetic braking control system.

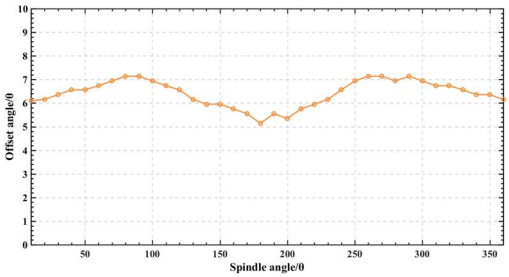

FIGURE 13. Brake slip at different angles of the spindle.

to it, and the step response curves of various algorithms after adding disturbance are obtained, as shown in Fig. 11. After adding disturbance, the traditional PID control has obvious oscillation, and it takes a long time to overcome the disturbance. Fuzzy PID also has small amplitude oscillation; The oscillation of the IBA-FNN PID control process is not obvious and can be overcome quickly, which shows that the IBA-FNN PID control algorithm has excellent disturbance compensation ability and anti-interference performance.

B. LOOM BRAKING EXPERIMENT

QJH910 rapier loom is used for the parking tests, and the braking control system is shown in Fig. 12. The industrial field control box controls the operation of the loom. The embedded main control module and electromagnetic braking module are integrated into the control box. The electromagnetic braking module carries out electromagnetic braking under the command and control of the main control module. The electromagnetic braking module acts on the electromagnetic clutch with the voltage signal and regulates the braking slip angle by adjusting the clutch excitation current.

Select the spindle angle ($10^\circ \sim 360^\circ$) to brake every 10° and measure the brake slip. The high-pressure braking time is 50ms, and the spindle speed is $500r/min$. The data of the braking angle slip test is shown in Fig. 13.

After braking at different positions in the loom movement, the angle fluctuation between the last stop position and the start braking position of the spindle is slight, and the average slip angle is 6.4°. According to the curve in Fig. 13, the braking process starts when the spindle angle is 180°, and

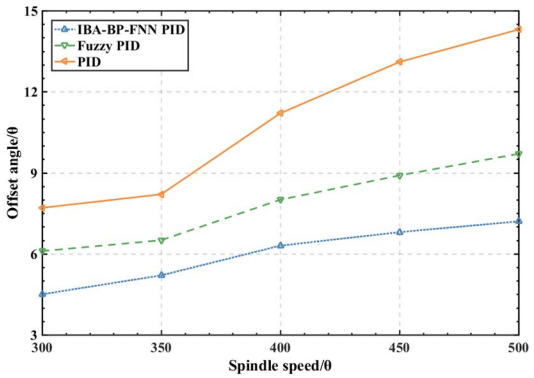

FIGURE 14. Positioning brake angle slip.

the corresponding angle change is the smallest, indicating that the spindle load at this position is large and acts in the same direction as the braking of the brake disc. When the spindle angle is 90° and 260°, the braking angle changes the most, indicating that the spindle load at this position is the smallest, so the braking angle changes the most.

When the loom speed is 300, 350, 400, 450, 500r/min, use PID, Fuzzy PID, IBA-BP-FNN PID to carry out 100 sets of positioning braking experiments at the warp breaking braking angle of 310°. Fig. 14 shows the braking Offset angle curve.

It can be seen from Fig. 14 that the braking slip angle is the largest in the PID control process, and the slip angle is also increasing with the increase of loom speed. The offset at 500r/min reaches 14.3°, which can not meet the demand of the loom within ±10°. It can be seen that the traditional PID control is difficult to change the parameters and the accuracy requirements of loom breaking under working conditions due to its limitations. Compared with PID control, Fuzzy PID control has smaller brake slip, and the slip will increase with the increase of speed, but compared with PID control, the fluctuation is relatively gentle, which shows that Fuzzy PID control has better adaptability. The slip angle range is 6.1° ∼ 9.7°, which can basically meet the accuracy requirements of braking. IBA-BP-FNN PID control has the minimum braking slip angle, and the range of slip angle is 4.5° ∼ 7.2°. With the increase in speed, the increase of slip is not obvious, so it has the optimal control ability. At the same time, because the positioning brake position is accurate, finding the braking angle is omitted in the positioning braking process, which significantly improves the production efficiency.

VI. CONCLUSION

Based on the operation technology of the loom, this paper deeply studies the electromagnetic clutch, discusses the factors affecting the braking accuracy of the loom, and improves the working performance of the braking system combined with an intelligent control algorithm. The braking control principle based on the excitation current, electromagnetic force, and torque of the electromagnetic clutch is obtained through the theoretical analysis of the mathematical model between the excitation current. According to the nonlinear and time-varying characteristics of electromagnetic braking system, a closed-loop control system of electromagnetic braking based on fuzzy neural network is designed on the basis of traditional PID control, which enhances the robustness and adaptability of the braking control system. The use of the IBA-BP fusion algorithm helps speed up the training speed of FNN and reduce the convergence error to obtain a more accurate control model. The electromagnetic braking experiment shows that FNN can effectively reduce the angle slip of loom braking and improve the braking stability under different working conditions compared with PID control and fuzzy PID control. The problems of uneven weft density and driving marks caused by frequent fluctuation of braking slip angle are avoided, and the fabric quality is improved. The system provides a possible solution to improve the control accuracy and stability of the loom braking system. At the same time, it also provides a reference for researchers engaged in the research of related textile equipment.

REFERENCES

[1] C. Dong, "Discussion on the development trend of rapier loom," *Mech. Manag. Develop.*, no. 1, pp. 41–42, 2012.
[2] M. Gao, W. Wang, Y. Zeng, Z. He, and C. Gao, "A rapier loom HMI system based on an easy cross-platform GUI software," in *Proc. 6th Int. Conf. Instrum. Meas., Comput., Commun. Control (IMCCC)*, Jul. 2016, pp. 874–878.
[3] Y. Yasa, E. Sincar, B. T. Ertugrul, and E. Mese, "A multidisciplinary design approach for electromagnetic brakes," *Electric Power Syst. Res.*, vol. 141, pp. 165–178, Dec. 2016.
[4] M. Kirchengast, M. Steinberger, and M. Horn, "Modeling and feedback linearization based control of an electromagnetic clutch actuator," in *Proc. IEEE Conf. Control Appl. (CCA)*, Oct. 2014, pp. 59–64, doi: 10.1109/CCA.2014.6981329.
[5] R. P. Borase, D. K. Maghade, S. Y. Sondkar, and S. Y. Pawar, "A review of PID control, tuning methods and applications," *Int. J. Dyn. Control*, vol. 9, pp. 818–827, Jul. 2020.
[6] M. Benosman, "Model-based vs data-driven adaptive control: An overview," *Int. J. Adapt. Control Signal Process.*, vol. 32, no. 5, pp. 753–776, May 2018.
[7] M. Cetin and S. Iplikci, "A novel auto-tuning PID control mechanism for nonlinear systems," *ISA Trans.*, vol. 58, pp. 292–308, Sep. 2015.
[8] Q. Zhao, R. He, and D. H. Hu, "Fuzzy PID control of the integrated system of electromagnetic brake and friction brake of car," *Adv. Mater. Res.*, vol. 988, pp. 568–575, Jul. 2014.
[9] X. D. Wang, T. W. Tu, and Y. Zhang, "Research on fuzzy control of electromagnetic clutch based on particle swarm optimization," *China Mech. Eng.*, vol. 21, no. 9, p. 1071, 2010.
[10] X. G. Wu, R. X. Liu, and N. N. Ding, "Genetic algorithm tuning PID control of magnetic powder clutch," *Adv. Mater. Res.*, vols. 712–715, pp. 2216–2222, Jun. 2013.
[11] D. Claudia-Adina, "An approach to fuzzy modeling of electromagnetic actuated clutch systems," *Int. J. Comput. Commun. Control*, vol. 8, no. 3, pp. 395–406, 2013.
[12] Y. Chen, C. Tu, and C. Lin, "Integrated electromagnetic braking/driving control of electric vehicles using fuzzy inference," *IET Electric Power Appl.*, vol. 13, no. 7, pp. 1014–1021, Jul. 2019.
[13] S. L. Li, Y. H. Du, and S. C. Yan, "Fuzzy self-adjusting PID control of electromagnetic clutch current," *J. Henan Univ. Sci. Technol. Natural Sci.*, vol. 31, no. 2, p. 4346 and 110, 2010, doi: 10.15926/j.cnki.issn1672-6871.2010.02.026.
[14] E.-L. Hedrea, R.-E. Precup, C.-A. Bojan-Dragos, E. M. Petriu, and R.-C. Roman, "Tensor product–based model transformation and sliding mode control of electromagnetic actuated clutch system," in *Proc. IEEE Int. Conf. Syst., Man Cybern. (SMC)*, Oct. 2019, pp. 1402–1407, doi: 10.1109/SMC.2019.8913909.

[15] C.-A. Dragos, S. Preitl, R.-E. Precup, E. M. Petriu, and A.-I. Stinean, "Adaptive control solutions for the position control of electromagnetic actuated clutch systems," in *Proc. IEEE Intell. Vehicles Symp.*, Jun. 2012, pp. 81–86, doi: 10.1109/IVS.2012.6232207.
[16] X. Wu, X. Wang, X. Xie, and T. Yu, "The single neuron PID controller for automotive electromagnetic clutch based on RBF NN recognition," in *Proc. Chin. Control Decis. Conf.*, Jul. 2008, pp. 2983–2987, doi: 10.1109/CCDC.2008.4597872.
[17] R. Yazdanpanah and M. Mirsalim, "Design of robust speed and slip controllers for a hybrid electromagnetic brake system," *IET Electr. Power Appl.*, vol. 9, no. 4, pp. 307–318, Apr. 2015.
[18] J. Pramudijanto, A. Ashfahani, and R. Lukito, "Designing neuro-fuzzy controller for electromagnetic anti-lock braking system (ABS) on electric vehicle," *J. Phys., Conf.*, vol. 974, Mar. 2018, Art. no. 012055.
[19] L. Quan, Z. B. Yang, L. Ding, and G. X. Huang, "Self-correcting fuzzy neural network control for the electromagnetic braking system of agricultural vehicles," *Trans. Chin. Soc. Agricult. Machinery*, vol. 12, pp. 122–125, 2005.
[20] P. V. de Campos Souza, "Fuzzy neural networks and neuro-fuzzy networks: A review the main techniques and applications used in the literature," *Appl. Soft Comput.*, vol. 92, Jul. 2020, Art. no. 106275.
[21] Y. Sun, J. Xu, G. Lin, and N. Sun, "Adaptive neural network control for maglev vehicle systems with time-varying mass and external disturbance," *Neural Comput. Appl.*, pp. 1–12, Mar. 2021.
[22] A. Salimi-Badr and M. M. Ebadzadeh, "A novel self-organizing fuzzy neural network to learn and mimic habitual sequential tasks," *IEEE Trans. Cybern.*, vol. 52, no. 1, pp. 323–332, Jan. 2022, doi: 10.1109/TCYB.2020.2984646.
[23] Y. Sun, J. Xu, H. Y. Qiang, and G. B. Lin, "Adaptive neural-fuzzy robust position control scheme for maglev train systems with experimental verification," *IEEE Trans. Ind. Electron.*, vol. 66, no. 11, pp. 8589–8599, Nov. 2019.
[24] J. Tavoosi, "An experimental study on inverse adaptive neural fuzzy control for nonlinear systems," *Int. J. Knowl.-Based Intell. Eng. Syst.*, vol. 24, no. 2, pp. 135–143, Jul. 2020.
[25] B. V. R. Kumar, K. Sivakumar, Y. S. Rao, and S. Karunanidhi, "Design of a new electromagnetic brake for actuator locking mechanism in aerospace vehcile," *IEEE Trans. Magn.*, vol. 53, no. 11, pp. 1–6, Nov. 2017, doi: 10.1109/TMAG.2017.2707242.
[26] I. V. Bochkarev and V. R. Khramshin, "Development of system for control of reversible electric drive friction-plate electromagnetic clutch," in *Proc. Int. Conf. Ind. Eng., Appl. Manuf. (ICIEAM)*, May 2017, pp. 1–5.
[27] D.-J. Li, Y.-Y. Li, J.-X. Li, and Y. Fu, "Gesture recognition based on BP neural network improved by chaotic genetic algorithm," *Int. J. Autom. Comput.*, vol. 15, no. 3, pp. 267–276, 2018, doi: 10.1007/s11633-017-1107-6.
[28] L. Chen, F. Zhang, and L. Sun, "Research on the calibration of binocular camera based on BP neural network optimized by improved genetic simulated annealing algorithm," *IEEE Access*, vol. 8, pp. 103815–103832, 2020, doi: 10.1109/ACCESS.2020.2992652.
[29] H. Pang, F. Liu, and Z. Xu, "Variable universe fuzzy control for vehicle semi-active suspension system with MR damper combining fuzzy neural network and particle swarm optimization," *Neurocomputing*, vol. 306, pp. 130–140, Sep. 2018.
[30] X. S. Yang, "A new metaheuristic bat-inspired algorithm," in *Nature Inspired Cooperative Strategies for Optimization*. Berlin, Germany: Springer, 2010, pp. 65–74.
[31] M. Rahmani, A. Ghanbari, and M. M. Ettefagh, "A novel adaptive neural network integral sliding-mode control of a biped robot using bat algorithm," *J. Vibrat. Control*, vol. 24, no. 10, pp. 2045–2060, May 2018.
[32] P. M. R. Bento, J. A. N. Pombo, M. R. A. Calado, and S. J. P. S. Mariano, "Optimization of neural network with wavelet transform and improved data selection using bat algorithm for short-term load forecasting," *Neurocomputing*, vol. 358, pp. 53–71, Sep. 2019.
[33] N. Aalimahmoody, C. Bedon, N. Hasanzadeh-Inanlou, A. Hasanzade-Inallu, and M. Nikoo, "BAT algorithm-based ANN to predict the compressive strength of concrete—A comparative study," *Infrastructures*, vol. 6, no. 6, p. 80, May 2021.

YANJUN XIAO received the bachelor's degree in industrial automation and the master's degree in machine manufacturing and automation from the Hebei University of Technology. He works as a Professor at the School of Mechanical Engineering, Hebei University of Technology. His research interests include waste heat recovery and industrial control.

XIAOLIANG WANG is currently pursuing the master's degree with the Hebei University of Technology. His major is electronic information. His research interests include embedded technology and intelligent control.

YUE ZHAO received the Graduate degree from Tangshan University, in 2021. She is currently pursuing the master's degree with the Hebei University of Technology. Her research interests include intelligent control and health management.

WEILING LIU is currently an Associate Professor with the School of Mechanical Engineering, Hebei University of Technology. Her research interests include intelligent and environmentally friendly instruments.